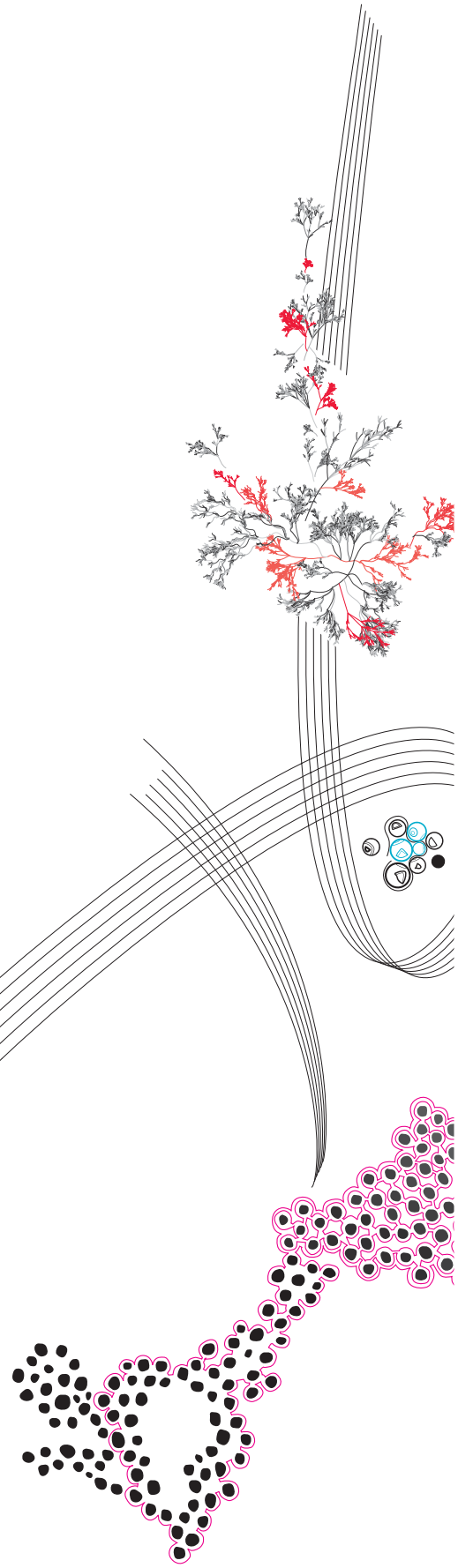

Bachelor Thesis

Optimizing a polydopamine coating protocol to adhere a hydrogel scaffold to a PDMS chip for application in a heart-on-chip model

D.A.G.B. Verhees

Daily supervisor: T. van Dorp, MSc
Commitee chair: Dr. A.D. van der Meer
External commitee member: Prof. dr. ir. P. Jonkheijm

July, 2022

Applied Stem Cell Technologies
Faculty of Science and Technology

UNIVERSITY OF TWENTE.

AST
APPLIED STEM CELL TECHNOLOGIES

Abstract

Heart-on-chip (HoC) devices are used to model the human heart and test drugs or research heart diseases. Heart diseases are the leading cause of death in the world, causing 16% of the world's total deaths in 2019. An ischemic heart exhibits a dysfunctional lymphatic network. However, there is no complete model with lymph and blood vasculature around the heart tissue. To integrate the vasculature an extracellular matrix (ECM) scaffold, such as hydrogel, is needed for support. Unfortunately, the hydrogel detaches from the walls of the microchip over time.

In this study, a polydopamine (PDA) coating is used to increase the hydrophilicity of the polydimethylsiloxane (PDMS) so the hydrogel stays attached. However, in the current coating protocol, the PDA solution is prepared with a Tris-HCl buffer under alkaline conditions (pH 8.5), which is fatal for the heart cells, since they only tolerate a neutral pH. This research focused on lowering the pH of the coating solution in which the DA is prepared without losing the ability to adhere the hydrogel to the PDMS in the chip.

Changing the alkaline Tris-HCl buffer to CM medium had the most positive impact on the micro engineered heart tissues (μEHTs), they never stopped beating after coating and encapsulation. Adding ammonium persulfate (AP) as oxidant seems to help the hydrogel stay attached in the chip for at least 4 days. The UV-vis spectrophotometry experiment showed that adding AP increases the amount of PDA intermediates formed. The water contact angle was 19°which indicates that the PDA coating in CM medium makes PDMS hydrophilic. The pressure experiment suggests that the hydrogel is better attached with a coating with the DA+AP in CM medium than in a Tris-HCl buffer.

Keywords: heart-on-chip, hydrogel, polydopamine coating, micro engineered heart tissue

Samenvatting

Hart-op-chips (HoCs) worden gebruikt om het menselijk hart te modelleren en medicijnen te testen of hartziekten te onderzoeken. Hartziekten zijn de belangrijkste doodsoorzaak ter wereld en veroorzaakten in 2019 16% van de totale sterfgevallen in de wereld. Een ischemisch hart vertoont een disfunctioneel lymfatisch netwerk. Er is echter geen compleet model met lymfe- en bloed vasculatuur rond het hartweefsel. Om het vaatstelsel te integreren is een extracellulaire matrix (ECM), zoals hydrogel, nodig voor ondersteuning. Helaas laat de hydrogel na verloop van tijd los van de wanden van de microchip.

In deze studie wordt een polydopamine (PDA) coating gebruikt om de hydrofiliciteit van het polydimethylsiloxaan (PDMS) te verhogen, zodat de hydrogel hecht. In het huidige coatingprotocol wordt de PDA-oplossing echter bereid met een Tris-HCl-buffer onder alkalische omstandigheden (pH 8.5), wat dodelijk is voor de hartcellen, omdat ze alleen een neutrale pH verdragen. Dit onderzoek was gericht op het verlagen van de pH van de coatingoplossing waarin de DA wordt bereid zonder het vermogen te verliezen om de hydrogel aan het PDMS in de chip te hechten.

Het veranderen van de alkalische Tris-HCl buffer naar CM medium had de meest positieve invloed op de micro ontworpen hartweefsels, ze stopten nooit met kloppen na het coaten en inkapselen met hydrogel. Het toevoegen van ammonium persulfaat (AP) als oxidator lijkt de hydrogel te helpen om minimaal 4 dagen in de chip te blijven zitten. Het UV-vis spectrofotometrie experiment toonde aan dat het toevoegen van AP de hoeveelheid gevormde PDA tussenproducten verhoogt. De water contacthoek was 19°, wat aangeeft dat de PDA-coating in CM-medium PDMS hydrofiel PDMS maakt. Het drukexperiment suggereert dat de hydrogel beter gehecht is met een coating met de DA+AP in CM-medium dan in een Tris-HCl-buffer.

Keywords: hart-op-chip, hydrogel, polydopamine coating, micro ontworpen hart weefsel

Contents

List of abbreviations

Abbreviation	Explanation
μEHT	Micro engineered heart tissue
AP	Ammonium persulfate
AST	Applied stem cell technologies
CF	Cardiac fibroblast
CM	Cardiomyocytes
CSP	Copper sulfate pentaphydrate
DA	Dopamine
DHI	5,6-Dihydroxyindole
DQ	Dopamine quinone
ECM	Extracellular matrix
HoC	Heart-on-chip
MI	Myocardial infaction
OoC	Organ-on-chip
PDA	Polydopamine
PDMS	Polydimethylsiloxane
SP	Sodium periodate

1 Introduction

1.1 Human heart

The human heart is the pump responsible for blood circulation. Without the heart blood would cease to flow and the human body would quickly die due to oxygen deficiency. The most prevalent types of heart cells are cardiomyocytes (CM) and cardiac fibroblasts (CF) [1]. Cardiomyocytes are the cardiac muscle cells which are responsible for generating contractile force [2]. Specialised CMs named pacemaker cells are responsible for controlling the rhythm of contractions [3]. CFs are responsible for producing and maintaining the extracellular matrix (ECM) [4]. The cardiac tissue is perfused with both blood and lymphatic vessels. Blood vessels are responsible for the delivery of oxygen and nutrients as well as he disposal of waste products [5]. Lymph vessels are needed for the regulation of tissue fluid homeostasis, by returning interstitial fluid via the vena cava to the heart [6]. Furthermore, the lymphatic system is responsible for the transportation of immune cells and the absorption of dietary fats [7].

Heart disease is the leading cause of death in the world, causing 16% of the world's total deaths in 2019 according to the World Health Organisation [8]. The absolute number has increased since 2000 by 2 million, bringing the total number of deaths to 8.9 million [8]. The most prevalent cardiovascular disease is ischaemic heart disease (46%) [9]. Ischaemic heart diseases are also called coronary heart diseases and describe heart problems caused by reduced blood flow to the heart muscle due to the gradual accumulation of atherosclerotic plaque in the blood vessels of the heart [9]. A dysfunctional lymphatic network is present in an ischemic heart [10]. However, there is no complete model with lymph and blood vasculature around the heart tissue. To better model the physiology and pathology of the heart it is necessary that the lymphatics are also taken into account. The cardiac lymphatics play a role in heart pathologies, such as atherosclerosis and myocardial infarction (MI) [6, 11]. In MI, commonly known as heart attack, the rapid death of CMs is caused by the lack of blood supply to the heart. MI also induces an increase in lymphatic capillaries and decrease in pre-collecting and collecting lymphatic vessels, which leads to a reduction in the cardiac lymphatic transport capacity [10]. This reduced lymphatic transport capacity, along with myocardial permeability, leads to fluid accumulation in the cardiac interstitial space, called myocardial edema [10].

Drugs being developed for heart diseases need to be tested on heart models. Unfortunately, in the last 30 years half of the drugs withdrawn from the market were due to cardiac toxicity [12, 13]. This calls attention to the limitations of the current drug-testing method in the oversimplified two-dimensional cultures of cardiomyocytes. A promising solution to this problem might be the relatively new and innovative organ-on-chip technology.

1.2 Organ-on-chip

The organ-on-chip (OoC) is a system that simulates the physiological environment of a human organ or at least the smallest functional unit of a organ [14, 15]. The system is a three-dimensional (3D) microfluidic device that contains a network of microchannels through which culture medium can flow to the 'organ', a micro tissue grown in the chip that can recapitulate tissue-specific functions [16].

1.2.1 Why organ-on-chip?

The need for a 3D culture environment arises from the poor representation of human physiology in 2D *in vitro* cell cultures [17]. The complexity of the physiological environment

cannot be reproduced in Petri dishes or well plates, since molecular gradients are missing, cell-cell and cell-matrix interactions are lacking and the production of ECM proteins can be reduced [18, 19]. However, the OoC strives to simulate the *in vivo* environment by replicating the 3D microarchitecture, the biochemical and mechanical microenvironment as well as organ functionality. Organ functionality is regulated by parameters such as the 3D ECM, tissue-boundaries, tissue-organ interactions, cell patterning, concentration gradients and mechanical forces such as compression, contraction and fluid shear stress [14, 20, 21]. This results in a more representative model of a human organ compared to 2D *in vitro* cell culture systems.

The OoCs representing different organs (e.g. liver, kidney, gut, lung, heart, vessel) can be used for toxicology research and drug discovery, testing and development [20, 21]. The expected future developments are improvements in toxicity assessments and development of treatments. Furthermore, the transition from the use of animal-based models to human-based models is a possibility [15].

1.2.2 Heart-on-chip

The heart-on-chip (HoC) device is an OoC system in which human heart tissue can be cultured [12]. Aside from the HoC a few other advancements were made, like the organoid models and bioprinted heart models [13]. However, organoid models cannot fully mimic heart physiology, because rhythmic mechanical stress and shear stress can not be applied as of yet [13]. On the other hand, the issue with bioprinting is that it is almost entirely dependent on the choice of the right bioinks [22].

A platform for generating and evaluating 3D engineered heart tissues was made by Ribeiro et al (2022) [23]. This platform was built for a 12 well plate, so it is not an on-chip device. But it was able to measure the force of contraction while under electrical and mechanical simulation.

Multiple papers have been published on HoC models, such as papers from Marsano et al (2016) and Abulaiti et al (2020). Marsano et al (2016) focused on mechanical stimulation of the myocardium [24]. They showed that stimulated micro-engineered cardiac tissues (µECTs) exhibit superior cardiac differentiation and promoted early spontaneous synchronous beating. Abulaiti et al (2020) focused on integrating a microelectromechanical system in the microfluidic chip where the 3D cardiac microtissues are cultured [12]. With many studies, the focus lies on electrical and mechanical stimulation, but more research on cardiovascular diseases would be interesting. This requires a combination of cardiac tissue and blood and lymphatic vasculature.

1.2.3 Blood and lymphatic vessels on chip

In the review paper by Ribas et al. (2016), multiple cardiovascular OoC platforms are mentioned [25]. However, in none of these OoCs were lymphatic vessels included. Only a small mention of the research by Sato et al. (2015) on vascular permeability was made where they used blood and lymphatic endothelial cells, but no heart tissue [26].

There are multiple studies in which OOCs were used to investigate lymphatic vessel functionality. For example, Gong et al (2019) created a 3D tubular microscale lymphatic vessel in a microchannel embedded in a collagen gel chamber [27]. They characterized the permeability and drainage of the lymphatic barrier and showed the potential for drug screening. The study showed the usefulness of the system as a disease model by modeling the tumor environment. In another study, lymphatic sprouting during the formation of new lymphatic vessels, termed lymphangionesis, was investigated by Kim et al (2016) [28].

When interstitial flow is generated over a fibrin hydrogel and different biochemical factors are applied, the lymphatic endothelial cells (LECs) are simulated to grow into the matrix channel on the microfluidic on-chip platform. So different aspects of the lymphatic system are being researched. Osaki et al (2018) combined lymphatic and blood vessels on chip and induced both lymphangiogenesis and vascular angiogenesis [29]. They observed different morphology in the junctions in the formed capillaries between the different cell types. They also tested several anti-angionetic factors. This model could be suitable for tumorigenesis models and drug screening assays for corneal disease.

1.2.4 Hydrogel as extracellular matrix

For the culturing of cells on a microfluidic chip hydrogels are often used as a 3D artificial ECM scaffold [19]. In a study from Lv et al (2016) it was observed that glioma cells cultured on a 3D scaffold showed more *in vivo* like proliferation than in a 2D culture [30]. The scaffold used provides the mechanical support and structural composition akin to the native ECM [30]. An example of a scaffold material is hydrogel. A hydrogel is a cross-linked polymeric network that has the ability to swell and retain water, but does not dissolve in water [31]. The reason why hydrogels are especially suitable as scaffolds is their flexibility, which is similar to native tissues, their mechanical stiffness and their porous network, which is suited for cellular organisation [31, 19].

The hydrogel matrix is excellent to use in an OoC, because it is able to mimic the ECM of specific organs due to the tunability of the elasticity, surface roughness and porosity [19]. In the microfluidic chip the nutrient supply and waste removal to the hydrogel, in which cells can be loaded and attached, can be regulated [19]. Additional advantages of using hydrogel in a chip are control over signalling gradients and temporal and spatial control over cellular distribution and fluids [19]. Examples of natural polymers that form biocompatible hydrogels are collagen and fibrinogen [19]. Collagen type 1 is commonly used as hydrogel scaffold for tissue engineering, because of the abundance of collagen present in the natural ECM, the ease of extraction and the adaptability [32]. Fibrin is a natural polymer that forms rapidly when thrombin is added to fibrinogen [19, 33]. The protease trombin (in the human body responsible for blood clotting) causes gelation of the hydrogel [33]. Often aprotinin is added as an antifibrinolytic agent to prevent hydrogel degradation [34]. The used hydrogel in vascular studies is often a combination of aforementioned hydrogels, because it offers the capability of tuning stiffness and structures [35]. Thus, a combination of specific hydrogels is an excellent substitution for the native ECM while heart cells are cultured in a microfluidic chip.

1.2.5 Material organ-on-chip device

In the development of OoC devices the used material for the chip is important. In order to have an optimal device, the following parameters need to be considered: gas permeability, non-toxic to cells, optical transparency and production costs [36]. Presently, inorganic materials (e.g. silicon and glass), elastomers (e.g. polydimethylsiloxane), plastics (e.g. polystyrene) and hydrogels (e.g. collagen) are being used in the fabrication of OoCs [13]. Of these options polydimethylsiloxane (PDMS) is the most widely used material for device fabrication due to its biocompatibility, optical transparency, simple fabrication and mechanical properties [37]. However, a major limitation of PDMS is its hydrophobicity (water contact angle $\approx 108° \pm 7°$) [38].

The mismatch between the hydrophobic PDMS and the hydrophilic hydrogel causes the hydrogel in the PDMS chip to detach from the channel walls, which can be seen in the

paper from Park et al (2019) [39]. The micro-engineered device they made for generation and culture of perfusable human blood vessels consisted of three parallel channels that were not completely separated. Vascular endothelial cells and fibroblasts were co-cultured in the central channel in a hydrogel scaffold. Without a coating the hydrogel detached and collapsed. Therefore it is essential to modify the PDMS surface to ensure proper attachment of the hydrogel in OoC applications. Limitations of many surface modification methods, like self-assembled monolayer (SAM) is that they require chemical specificity between modifier and surface, however, this is not the case for polydopamine (PDA) [40].

1.2.6 Polydopamine coating

Lee et al (2008) have reported a method to form multifunctional polymer coatings inspired by mussels, which have the ability to attach to practically all types of surfaces [41]. The foot protein of mussels contains 3,4-dihydroxy-L-phenylalanine (DOPA) and lysine amino acids. The catechol and amino functional groups present in these amino acids can form covalent and noncovalent interactions with substrates [42]. Dopamine (DA) has both these functional groups and utilizes the same binding mechanism. DA can self-polymerise to form a PDA coating on various surfaces. However, researchers are not in agreement on the mechanism of PDA formation and what the end product is: noncovalent assemblies, heteropolymer, oligomers and/or trimers [40]. Nevertheless, they do agree that the driving force is most likely the oxidation of DA by dissolved oxygen in an alkaline solution [40]. One of the proposed pathways can be seen in Figure 1, where the formation of different compounds changes the colour of the solution from transparent to yellow to orange/red to finally a deep brown blackish coluor, see Figure 1 [43].

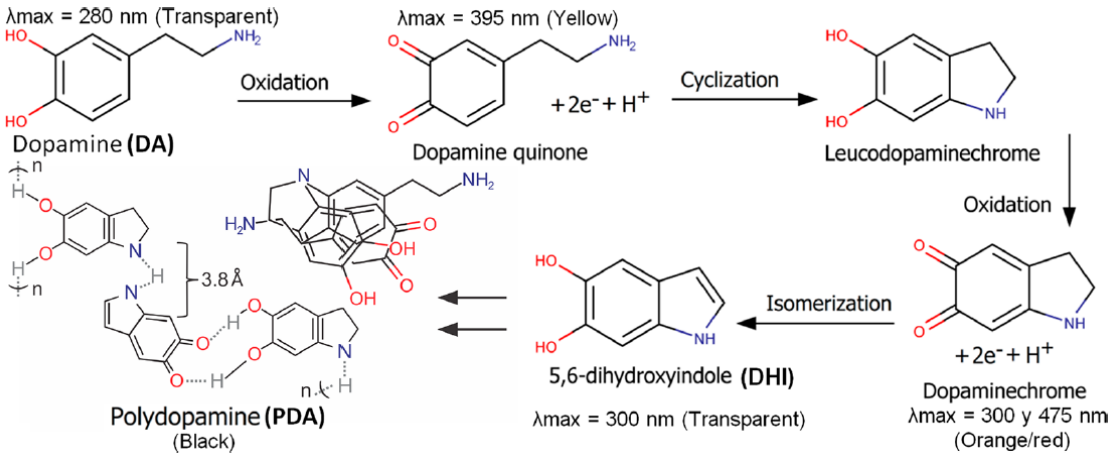

Figure 1: Stepwise polymerization of dopamine into polydopamine, and the corresponding wavelengths of the colour changes [43].

An unique charactersistic of PDA coatings is the ability to deposit a thin film onto practically all types, sizes and shapes of (in)organic surfaces. The process is simple: dipping the surface in an alkaline solution in which PDA is present. The original method of Lee et al uses 2 mg/mL of dopamine hydrochloride dissolved in a 10 mM Tris-HCl buffer at pH 8.5 [41]. This creates a 50 nm thick layer of PDA on the surface in 24 hours. After Lee's publication in 2007, more research was done to optimise the speed of the coating process [44]. Variables that influence the coating speed are the concentration of DA, pH of the buffer and addition of oxidants [44].

There are several options to help the oxidation of DA to dopamine quinone in neutral conditions in the PDA Tris-HCl solution by addition of oxidants like: ammonium persulfate (AP), sodium periodate (SP) and copper sulfate pentaphydrate (CSP) or by the addition of the element vanadium [45, 46, 47, 48]. The most promising oxidant is ammonium persulfate (AP), because Wei et al (2010) showed that when added to DA under weak acidic, neutral or weak alkaline conditions PDA was formed [45]. They tested different molar ratios of DA to AP and they got the most PDA formation at 2:1 [49]. Other tested oxidants work very slowly at a pH of 7 (SP) or have not yet been tested with a pH of 7 (CSP), so they are less promising [46, 47]. Furthermore, vanadium is used to modify hydrogels and is not used as a coating in the paper of Park er al [48]. The optimization of PDA coating was not performed on living cells, so it is unpredictable if these options only lower the pH or also have a negative influence on the heart tissue in the microchip, this will be tested in this research.

2 Research plan

To integrate the lymphatic vasculature in the HoC model, hydrogel is used as ECM scaffold for the blood and lymphatic vessels to grow in. Unfortunately, the hydrogel detaches from the walls of the chip over time [39]. A PDA coating can be used to increase the hydrophilicity of the PDMS. In the current coating protocol, the DA solution is prepared with a 10 mM Tris-HCl buffer under alkaline conditions (pH 8,5) based on the aforementioned research of Lee et al [41]. For the application in the heart-on-chip this is fatal for the heart cells (CMs and CFs), since they only tolerate a pH around 7.

This research will focus on bringing down the pH of the coating solution in which the DA is prepared without it losing the ability to adhere the hydrogel to PDMS in the chip. First, the effect of lowering the pH and adding the oxidant AP will be analysed with ultraviolet–visible (UV-vis) spectrophotometry to determine if and how fast PDA is formed. Water contact angle measurements will determine whether the PDA coating lowers the hydrophobicity of PDMS, which would suggest better hydrogel adhesion. Testing the adhesion of the hydrogel to the PDA coated PDMS surface will be done in a 3D microfluidic chip environment. By applying air pressure, the strength of the hydrogel attachment in the channel of the chip will be evaluated. The best coating conditions will then be tested on CMs with a PrestoBlue metabolic activity assay to get an indication of the toxicity of the coating. Finally, the effect on the μEHT in the microchip will be tested and evaluated under the microscope.

The expectation is that by adding AP the PDA reaction changes from alkaline pH-induced DA polymerization to AP-induced DA polymerization [45]. This would mean the pH of the coating solution can be neutral, which is better for cells. Still the most and fastest DA polymerization will happen at alkaline pH, but adding AP will also make it possible at lower pHs [45]. As for the water contact angle; the PDA makes the PDMS hydrophilic (contact angle between 50-60%) [39]. The AP only induces the DA polymerization. So the assumption is that AP in itself does not influence the contact angle. The hydrogel adhesion to DA+AP coated PDMS chip channels will be best when the buffer has a pH of 8.55, but lower a pH will also work as long as AP is added. For cell viability, the expectation is that the metabolic activity is low when a coating with high pH is added. The neutral PDA buffer solution will be better for the cells. For last experiment the expectation is that the adhesion of hydrogel and the viability of heart cells depends on which conditions are chosen. The conditions with a high pH, will damage the heart tissue, but the hydrogel will adhere. For the conditions with a neutral pH, the heart tissue is expected to survive, but if the hydrogel attaches is as of yet unknown.

3 Materials and methods

3.1 PDMS chip fabrication

PDMS solutions were prepared by mixing the silicone elastomer base and the silicone elastomer curing agent (SYLGARD ^{TM} 184, 1272/2008) in a weight ratio of 10:1. The flat slabs of PDMS were made by casting the PDMS solution into a petri dish (Greiner bio-one, 664160). The straight channel microchips were made by casting PDMS on a micromilled PMMA mold. The dimensions of the channels in the chip are: 51 μm x 300 μm x 14 mm (height x width x length). The cell culture chambers in the μEHT chip have these dimensions: 1 mm x 1mm x 6 mm. The molds containing the top layer of the chip with PDMS were degassed in the desicator until all air bubbles were removed. After which it was placed in the oven for heat-curing at 65°C. The bottom layer of the chip is made by spin coating a thin layer of PDMS onto a microscope slide (Epredia, ISO 8037/1) with the spin coater (SPS, Spin 150) and heat-curing it in the oven. After that, the two layers were bonded in the Plasma System (Femto Science, CUTE). The chips were checked for air bubbles and blockage in the channel under the microscope.

3.2 Polydopamine coating

The DA solutions were made by dissolving 2 mg/mL dopamine hydrochloride (DA) (Sigma-Aldrich, H8502) in a 10 mM Tris-HCl buffer with pH 8,55. The Tris-Hcl buffer was titrated using HCl to obtain pH valuse of 7.93; 7.51; 7.06; 6.87; 5.90; 2.61. The oxidant ammonium persulfate (Sigma-Aldrich, 215589) was added in the ratio 2:1 (DA:AP).The coating time was varied between 30 minutes and 2 hours.

3.3 UV-vis spectrophotometry

The UV-vis recording spectrophotometer (Shimadzu UV-2401 PC) was used to measure the absorbance intensity of the DA polymerization for 3 hours at an interval of 30 minutes under the different conditions. The cuvettes (Greiner bio-one, 613101) were filled with 1 mL of DA and/or AP in a Tris-HCl solution or in CM medium (components in Appendix 8.1). The solutions were referenced to the Tris-HCl buffers/CM medium to see change caused by DA polymerization.

3.4 Contact angle measurements

The optical contact angle of a 2 μL water droplet on differently coated PDMS surfaces was measured using the sessile drop method of the optical contact angle measuring and contour analysis system (Dataphysics, OCA20).

3.5 Hydrogel attachment

The 4 channels in the chip were coated with DA or DA+AP dissolved in either a Tris-HCl buffer or in CM medium for 60 min. For the Tris-HCl buffers pHs of 8.55 and 7.51 were used and the CM medium has a pH of 7.3. After coating, the hydrogel was made by mixing 3 mg/mL Fibrinogen, 0.2 mg/mL Collagen I, 3.75 μg/mL Aprotonin and 0.9 U/mL Thrombin in PBS (Thermo Fisher Scientific, 14190250) (Appendix 8.3). A volume of 2 μL hydrogel was inserted per channel. After 15 min of gelation the chip was connected to the modular pressure-based flow controller (Fluigent, FLOW EZ). The applied pressure was increased until the hydrogel detached and appeared at the outlet.

3.6 Cell culture and PrestoBlue metabolic activity assay

For the metabolic activity assay, a multiwell cell culture plate with 96 wells (VWR, 10062-900) was used to culture hPSC-derived CMs (DRRAGN). The hPCSs were differentiated following the protocol described in the article by Ribeiro et al. (2020) [50]. The plate was coated with 1% Vitronectin (Thermo Fisher Scientific A31804) in PBS ratio 1:100 for 30 minutes at room temperature. After which CMs were thawed and DMEM (Thermo Fisher Scientific, 31331093) was added and centrifuged at 240g for 3 minutes. CMs were diluted with CM medium to 400000 cells/mL. The components of the CM medium are listed in Appendix 8.1. Per well 100 μLcell suspension was added and incubated overnight at 37°C.

Six coating conditions were chosen to test their effect on the CMs: DA with and without AP in Tris-HCl pH 8.55 and pH 7.51 and in CM medium pH 7.3. The controls with cells were: CM medium (positive control) and saponin (Sigma-Aldrich, S7900-25G) (negative control). The other controls were: only AP in CM medium and CM medium with PrestoBlue (10:1) without cells. Coating times of 30 minutes, 1 hour and 2 hours were tested. The PrestoBlue HS Cell Viability Reagent (Thermo Fisher Scientific, P50200) and the CM medium mix (ratio 1:10) were added to the wells and incubated for 30 minutes at 37°. Then the mix was pipetted in a Sterilin Black microtiter plate (Thermo Fisher Scientific, 611F96BK) and read by the Multilabel Plate Reader (PerkinElmer, VICTOR3) at wavelengths 560 nm and 590 nm . This metabolic assay was done at 0h, 2h, 4h and 24h after the coating to look at possible recovery of the CMs.

3.7 Seeding of µEHT and hydrogel encapsulation in microchip

The μEHT chips were first coated with 1% Pluronic F-127 (Sigma-Aldrich, P2443-250G) to make the channel walls extra hydrophobic, so no cells adhere. The CMs and CFs (Bio-Connect, cFBs) were mixed in medium in the ratio 9:1. Per chip 650000 cells are required. The cell-gel mixture was made, by mixing the cell medium with 2 mg/mL Fibrinogen, 1 mg/mL Matrigel, 2.5 μg/mL Aprotonin and 0.6 U/mL Thrombin, see Appendix 8.2. This cell-gel mixture was pipetted into the chambers of the the chip, were the gel polymerized for 10 minutes. After which the channels of the chip were filled with medium by inserting pipet tips in the reservoirs.

On day 7 the chips were coated before encapsulation of the tissue with hydrogel. The channels were washed 3 times with PBS, before and after the coating. The PDA coating solution was made following section 3.2. For the hydrogel 3 mg/mL Fibrinogen, 0.2 mg/mL Collagen I, 3.75 μg/mL Aprotonin and 0.9 U/mL Thrombin is mixed in CM medium. Polybead 10 μm microspheres (Polysciences, 17136-5) were added to visualise the hydrogel under the microscope. The hydrogel was then inserted into the chip chambers and after 10 to 15 minutes of gelation, medium was added to the chip channels. The encapsulated tissues were imaged daily to monitor the effect of the coating on μ EHT and to observe the attachment of the hydrogel.

4 Results

4.1 UV-vis spectrophotometry

The UV-vis spectra of the DA polymerization reaction were measured to quantify the PDA intermediates formed. The first product that is oxidized is DA quinone, which absorbs light at a wavelength of 300 nm. DA oxidized in Tris-HCl buffer with a pH of 8,55 results in the highest formation of DA quinone, as the peak in Figure 2a indicates. The same applies to AP-mediated DA oxidation (DA+AP), only the peak is higher and broader, as can be seen in Figure 2b. The intermediate DHI is formed at a wavelength of 395 nm and this quantity is also highest with a Tris-HCl buffer with pH 8,55. The DA+AP oxidation reaction differs from the DA oxidation in two aspects: the absorption intensity of at least the intermediates is higher and the visible colour change differs. The addition of AP results in orange/red colours, see Figure 2d. While the DA polymerization gives more greyish colours as can be seen in Figure 2c. The UV-vis spectra and colour change over time for each condition can be found in Appendix 8.4.

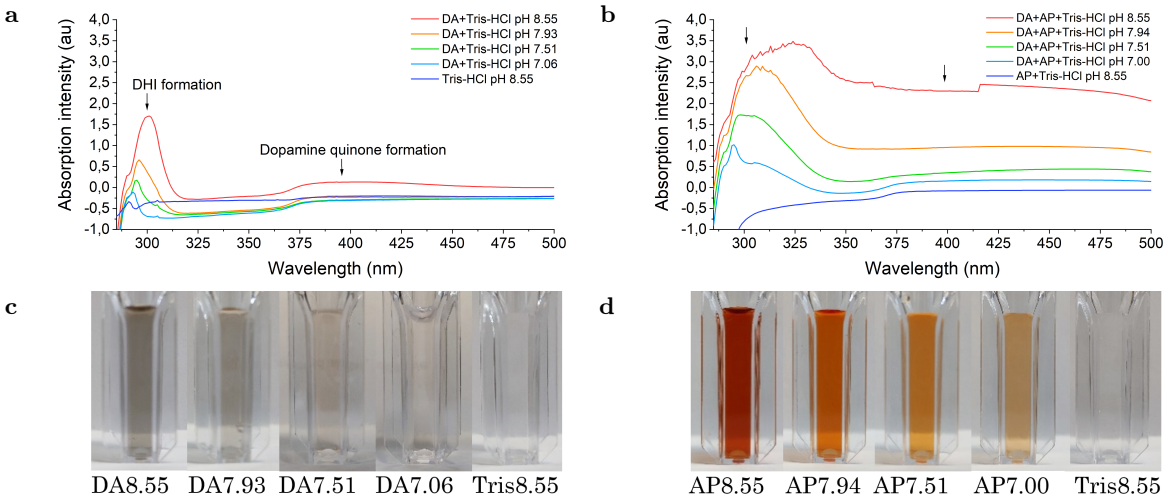

Figure 2: UV-vis spectra **(a)** and colour change **(c)** at 60 minutes of DA in various Tris-HCl pH buffers. UV-vis spectra **(b)** and colour change **(d)** at 60 minutes of DA+AP in various Tris-HCl pH buffers. The formation of intermediates DHI and DA quinone at 300 and 395 nm respectively is indicated by arrows. n=3

Changing the buffer solution from Tris-HCl to CM medium resulted in high absorption intensities for intermediates in the DA+AP oxidation reaction, see Figure 3a. The final product of the polymerization reaction is PDA, which is black. This colour was formed in the DA+AP oxidation reaction, see Figure 3b.

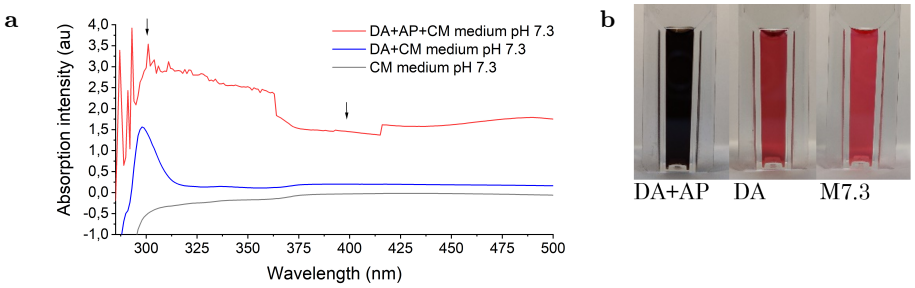

Figure 3: UV-vis spectra **(a)** and colour change **(b)** at 60 minutes of DA and DA+AP oxidation in CM medium. The arrows indicate that at wavelength 300 nm the intermediate DHI is formed and at 395 nm DA quinone is formed. n=3

The most DA quinone intermediate and therefore presumably PDA is formed in the first hour for the DA+AP oxidation in Tris-HCl pH 8,55 or CM medium, see Figure 4. After 45 minutes to an hour, the increase is discontinued. For DA oxidation, the increase in DA quinone is almost linear and increases slowly over time.

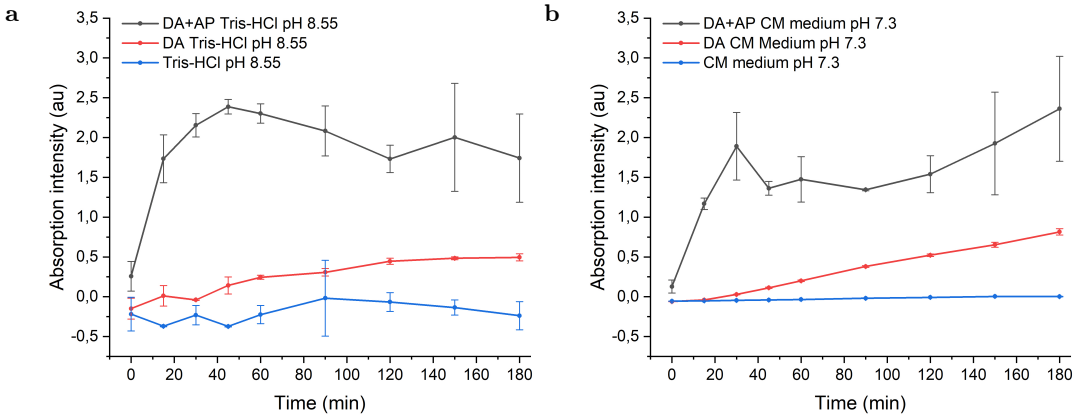

Figure 4: Absorption intensity **(a)** at 395 nm (DA quinone) of DA (red) and DA+AP (black) in a Tris-HCl buffer pH 8.55 and control of only the buffer (blue) over 3 hours time. Absorption intensity **(b)** at 395 nm (DA quinone) of DA (red) and DA+AP (black) in CM medium pH 7.3 and control of only the CM medium (blue) over 3 hours time. Dots represent mean ± SD. n=3

4.2 Contact angle measurements

The contact angle of water on differently coated PDMS surfaces was measured to determine the hydrophilicity of the surface. The measured water contact angle of the uncoated PDMS is 113°, see Figure 5. The contact angle of the PDMS surface coated with DA in a Tris-HCl buffer with pH 8.55 is significantly reduced to 56°. The coating DA+AP in Tris-HCl with pH 8.55 also caused a lower contact angle (98°) compared to uncoated PDMS, but caused a significantly higher contact angle than the DA coating. Coating of DA or DA+AP in a Tris-HCl buffer with a pH lower than 8.55 has no influence on the water contact angle, see Figure 19 in Appendix 8. The combination DA+AP also has no significant effect for Tris-HCl buffer with a pH of 7.51 compared to PDMS, see Figure 5. The CM medium coatings have the opposite effect than the Tris-HCl buffer with pH 8.55, because the PDMS surface with the DA+AP coating has a significantly lower contact angle than the DA coating, see Figure 5. The mean water contact angles are 19°and 93°, respectively.

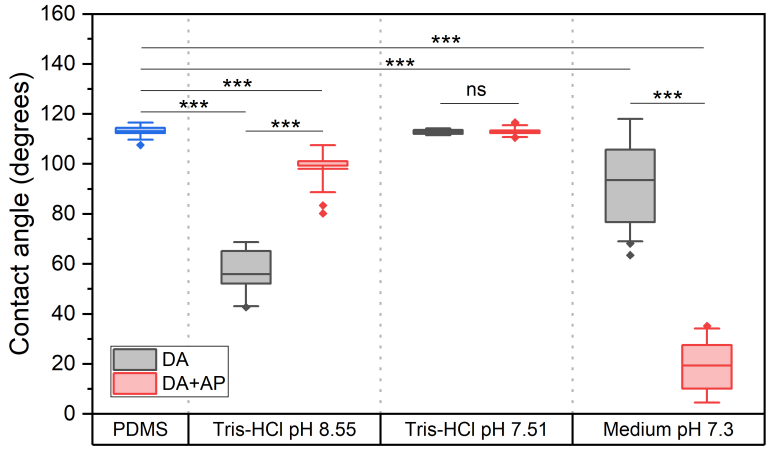

Figure 5: Water contact angle measured on uncoated (blue) and coated PDMS surfaces. The used coatings were DA (black) and DA+AP (red) in Tris-HCl buffers with a pH of 8.55 and 7.51 and CM medium with a pH 7.3. The error bars represent SD and the diamond shapes mark the outliers. *p $<$ 0.05, **p $<$ 0.01, ***p $<$ 0.001 and ****p $<$ 0.0001. n=12

4.3 Hydrogel attachment

The attachment of the hydrogel to the PDMS was evaluated by applying pressure on hydrogel inside a straight channel. The variation in the hydrogel attachment experiment was very large as can be seen in the size of the error bars in Figure 6. The coefficient of variation is between 14% and 47%. Therefore, the coating conditions have no noteworthy effect on the hydrogel attachment compared to the uncoated chip.

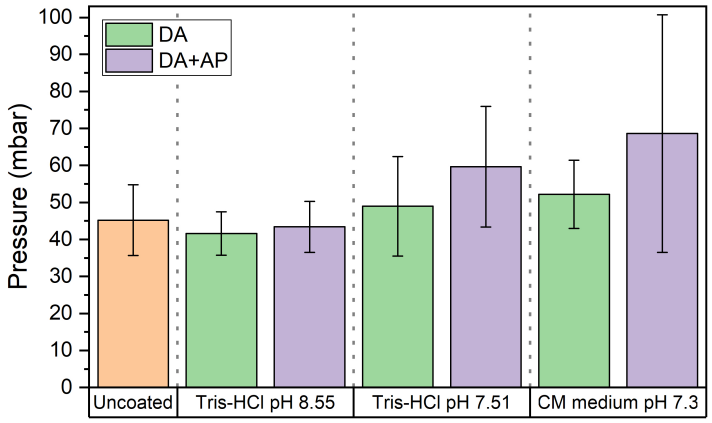

Figure 6: Amount of pressure at which the hydrogel detaches from the channel under different conditions: no coating (orange), coated with DA (green) or DA+AP (purple) in Tris-HCl buffers with a pH of 8.55 and 7.51 and CM medium with a pH of 7.3. Bars represent mean ± SD. n=4

4.4 PrestoBlue metabolic activity assay

The toxicity of the different coatings was evaluated by performing a PrestoBlue assay to determine the metabolic activity of the cells after coating. The positive and negative controls in the metabolic assay gave approximately the same fluorescence values. So the CMs in CM medium and the CMs in saponin had the same amount of reducing cell activity. Only the conditions in CM medium showed more fluorescence directly after the coating,

especially with only DA, see Figure 7a. However, 24 hours after coating there was no noteworthy difference anymore.

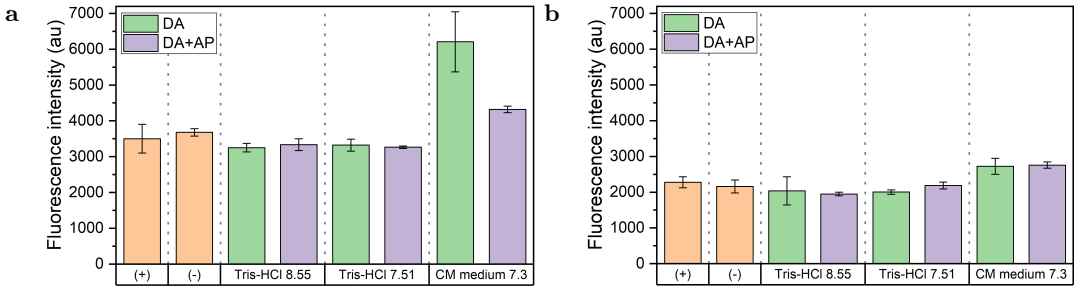

Figure 7: Fluorescence intensity of the PrestoBlue metabolic activity assay under different coating conditions measured at 0 hours **(0)** and 24 hours **(b)** after coating. The orange bars are the controls: positive (+) and negative (-). Bars represent mean ± SD. n=3

In both positive and negative control wells there were CMs before the PrestoBlue assay was done, but no more after, see Figures 8a,b,d,e. After the DA in CM medium coating there were very few CMs remaining, see Figure 8f.

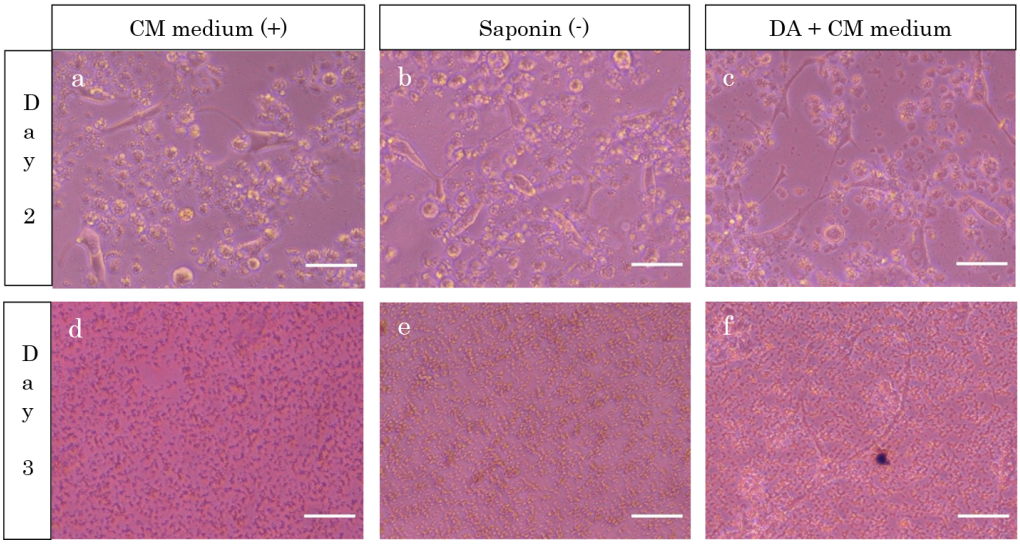

Figure 8: Microscope pictures taken of the CM monolayer in the 96 wells plate under different conditions. On day 2 **(a-c)** CMs, dead cells and debris was seen. On day 3 **(f-h)** the PrestoBlue assay was done and only debris was seen, except for the DA in CM medium **(f)** condition. Scale bars: 50 μm.

4.5 Encapsulation of µEHT in microchip

The effect of different coatings was evaluated by adding it to the microchips and monitoring the whether or not theμEHTs were beating and whether the hydrogel stayed attached to the chamber wall or detached. The μEHTs were all beating before the coating was added and they were encapsulated by hydrogel on day 7. Right after encapsulation the tissue that were coated with DA or DA+AP in a Tris-HCl buffer stopped beating. Only DA in Tris-HCl with a pH of 8.55 recovered and started beating again, but the hydrogel started to detach after 15 days. These tissue were monitored for 21 days and the other tissues only

Conditions	Day 7		Day 11		Day 21	
	Tissue beating	Hydrogel attached	Tissue beating	Hydrogel attached	Tissue beating	Hydrogel attached
No coating	4/4	4/4	4/4	0/4		
DA Tris-HCl pH 8.55	0/3	3/3	1/3	2/3	3/3	0/3
DA+AP Tris-HCl pH 8.55	0/3	3/3	0/3	3/3	0/3	2/3
DA+AP Tris-HCl pH 7.51	0/3	3/3	0/3	0/3		
DA CM medium	2/2	2/2	2/2	1/2		
DA+AP CM medium	4/4	4/4	4/4	3/4		

Table 1: Overview with whether the tissue where beating or not and whether the hydrogel was attached to the chamber wall or detached under different conditions. On day 7 the tissues were encapsulated. In Figure 9 the images can be seen.

for 11 days. The hydrogel in the control chip without coating started to detached on day 9, so only 2 days after encapsulation.

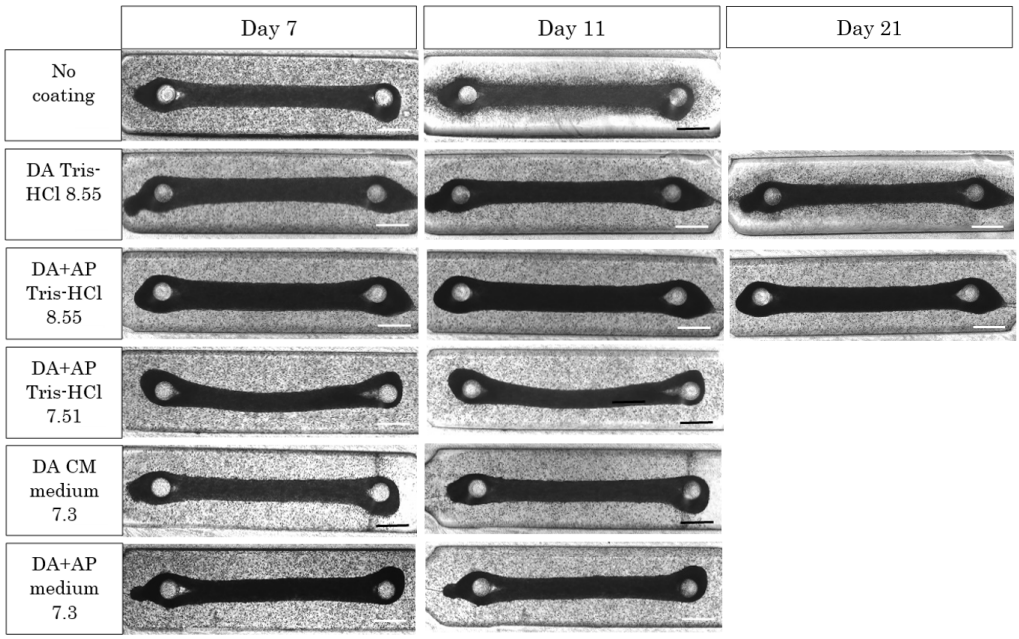

Figure 9: Images of the μEHTs cultured on chip. On day 7 the chips were coated and the tissues were encapsulated with hydrogel with beads. Tissue were uncoated, coated with DA and DA+AP in Tris-HCl with pH 8.55 for 30 minutes, DA+AP in Tris-HCl with pH 7.51 for 60 minutes and DA and DA+AP in CM medium pH 7.3. Note that on day 11 for only 2 conditions the hydrogel detached: no coating and DA+AP in Tris-HCl pH 7.51. Scale bars: 500 μm.

5 Discussion

The UV-vis spectra show that at both DA and DA+AP in an alkaline pH solution there is more and faster formation of the PDA intermediates than at lower pHs, as expected. However, the spectra of DA+AP oxidation differ from those of Wei et al. [49]. They saw an absorption peak at 300 nm and one at around 350 nm. In the UV-vis experiment only a broader peak around 300 nm was noticed in Figure 16b. This difference is caused by the difference in pH (4 for Wei and 8.55 here) and running time (1500 min for Wei and 180 min here). The absorption intensity line graph at 395 nm for the DA+AP oxidation was very similar to what Lamaoui et al (2021) measured at 420 nm over time [51]. In both the absorption did not further increase after 45 minutes. So it would be useful to test the effectiveness of shorter coating times in the future.

The contact angle of the PDA coated PDMS surface is comparable to the results of similar studies by Park et al (2019), Wei et al (2010) and Chuah et al (2015) [39, 45, 52], namely between 50% and 60%. However, the results from DA+AP were unexpected. In the Tris-HCl buffer with a pH of 8.55 they were higher and in the CM medium they were lower than only the DA. So it seems that AP can bring the contact angle either up or down depending on the solution in which it mediates DA to polymerize. In CM medium a lot of different components are present that may have had an influence. However, in the control with only a medium coating the contact angle was the same as for PDMS, see Figure 19 in the Appendix. This means that the components on there own have no effect, but it is possible that they bind to the dopamine coating. That would explain why the contact angle for DA in CM medium is 93°instead of around 50°. It is unexpected that the DA+AP in Tris-HCl buffer with pH 8.55 has a higher contact angle than only DA, because looking at the UV-vis results there should be more PDA. In the papers from Wei et al they also didn't do contact angle measurements on PDMS. So it is unclear how the AP should affect the contact angle. Ponzio et al (2016) did use DA+AP, but they coated silicon wafers, not PDMS [53]. The contact angle was approximately 20°. This is the same as the contact angle found in CM medium. The PDMS slabs were coated by letting them float upside down in the coating solution. This could mean that the formed PDA floats to the bottom and does not fully functionalize the PDMS surface.

In the hydrogel attachment pressure test the standard deviations were very high. This means the results are not reliable. It would seem that the DA+AP coating can withstand higher pressures, but this is not certain because of the large error bar. For further research the sample size should be increased. Also the protocol needs to be improved. In this study the hydrogel got also in the reservoirs. This meant that sometimes the channel was already empty, but hydrogel got stuck in the reservoir. The values in the graph are the pressures when the hydrogel appears at the outlet. Thus, the hydrogel in the reservoirs can increase the resistance. However, this should be the same for all channels, because the same hydrogel volume was used. My recommendation is to use the same design as the chips for the μEHT, but with only one chamber. The advantage of this is that due to the narrowing channel parts the hydrogel can be loaded in the chamber only. Also the experiment was done right after the hydrogel gelated. But as was seen in the last experiment with de μEHTs on chip the hydrogel only started to detach 2 days after encapsulation. When the pressure test is also be done days after encapsulation, the expectation is that the results will differ more between conditions.

In the PrestoBlue metabolic activity assay an indication of the toxicity was tried to be acquired. PDA does not hinder the viability or proliferation of mammalian cells such as fibroblasts according to Ku et al (2010) [54]. Also PDA can even be used for stem

cell adhesion [52]. However, in these papers the surface was first coated with PDA after which the cells were added. Therefore, this does not say anything about the toxicity of the coating solution. About the cytotoxicity of Tris-HCl on cardiomyocytes there is no information. But in general a pH higher or lower than 7.3-7.4 reduces the cell viability [55]. Regarding DA+AP conditions, cell death could be caused by AP. Kašpárková et al (2019) researched the cytotoxicity of an ammonium persulfate solution (AP dissolved in culture medium) on mouse embryonic fibroblast cells [56]. They discovered that an AP concentration of 1 mg/mL resulted in cell viability of 50%. According to the international standard EN ISO 10 993-5 this value is assigned to moderate cytotoxicity. In Figure 7a it was seen that cells coated with DA+AP in CM medium had a higher fluorescence value than the DA medium coating. This could indicate a higher cell viability. However, the positive and negative control had the same fluorescence value, so the results are not reliable. For further research, the PrestoBlue metabolic activity assay should be performed again. Factors that could be changed to try to get better results are longer maturation of CMs, less wells and pipetting more carefully. By culturing the CMs longer before adding the coating, the cells are closer in age to the cells in the μEHT on chip. The washing steps take a lot of time for 63 wells, during that time the cells are without medium. So, by taking care of fewer wells everything will be done faster and more time can be taken for pipetting precise volumes. Also it is worth investigating what using less AP would mean for the formation of PDA and the cell viability. A concentration of 0.5 mg/mL meant only mild cytotoxicity on fibroblasts for Kašpárková et al [56]. So the expectation is that also for cardiomyocytes the cell viability would be better.

For the last experiment, all aspects were joined by adding the coating before hydrogel encapsulation to the μEHTs on chip. The hydrogel stayed attached for at least 11 days in the chip channel when the DA was prepared in a Tris-Hcl buffer with a pH of 8,55 as expected based on the study by Park et al (2019) [39], who showed that the hydrogel attaches in square shaped PDMS wells if they are PDA treated. Some tissues were only followed for 11 days due to a lack of time. Only 2 chips were coated before the others, so of them there are also results at day 21. It was unexpected that the μEHTs are more negatively affected by the lack of medium components than by the high pH. Because in Table 1 the tissues coated with DA or DA+AP in CM medium kept beating, but the tissues coated in Tris-HCl buffer with approximately the same pH stopped beating. It could be that pH is not the killing factor, but the lack of medium components is. This needs to be investigated further.

5.1 Further research

The μEHT should be tracked over a longer period of time to see if the hydrogel detaches. The hydrogel attachment experiment did not work well. For future research, a different chip can be used, see Figure 10. The chip has three inlets and three outlets. In the channel in the middle, the hydrogel will be loaded, and because the row of triangles that offer resistance the hydrogel will not enter the adjacent channels. To evaluate whether or not the hydrogel attaches to the PDMS, a fluorescent dye will be added in one side channel. If the hydrogel is attached to the PDMS, the fluorescent dye will stay in that side channel. If not, the dye will leak through the middle channel into the other side channel. This situation is more comparable to the HoC application for which the coating is being optimized. A comparable experiment was conducted by Park et al (2019) [10], they used the fluorescent FITC-dextran to observe if their engineered blood vessels can be perfused. The intravascular flow was visualised with a Zeiss LSM 800 confocal microscope. However, for this experiment only the leakage from the possibly detached hydrogel has to

be visualized. So an EVOS fluorescence microscope has a resolution high enough to see if the FITC-dextran dye leaks past the detached hydrogel. The molecular weight should be high to prevent the dye solution from simply being able to pass through the hydrogel.

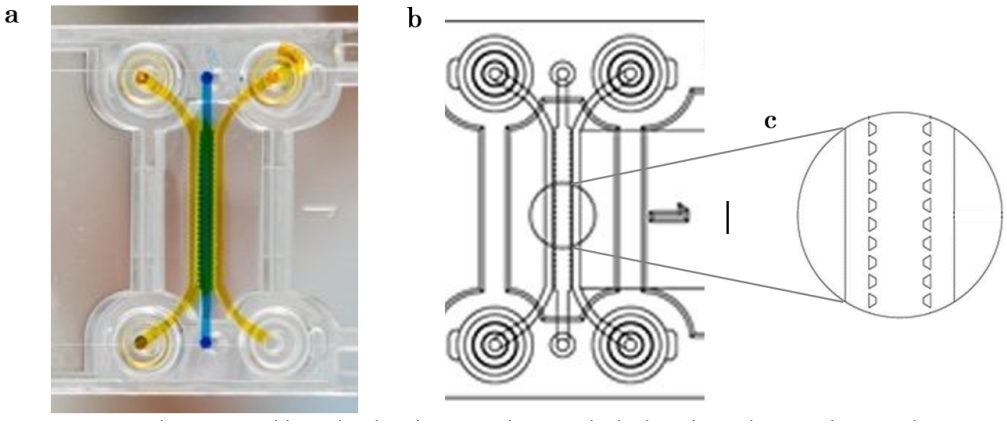

Figure 10: Microchip image **(a)** and schematic **(b)** comparable to the chip that can be used to test the hydrogel attachment. The triangles **(c)** prevent the liquid in the three channels from mixing [57].

An unanswered question is what exactly happens with DA polymerization in medium. What influence do the medium components have. To gain in-depth knowledge of the surface morphology of the PDA coatings, field emmision scanning electron microscope (FESEM) pictures should be taken. FESEM can show if the coated PDA layer was composed of aggregated nanoparticles like in the paper from Wei et al (2010) [45]. FESEM can also reveal if medium components adhere to the PDA coating.

When the PDA coating protocol is fully optimized it can be used attach the hydrogel in the chip and future research can try to let blood and lymphatic vasculature grow in the hydrogel. The PDA coating will be applicable not only in the HoC, but also in various other applications because chemical specificity between the modifier and the surface is not needed with PDA. And because the modification in the protocol the coating will also be suitable to be used in cell environment.

6 Conclusion

The aim of this research was to optimize the PDA coating protocol so that the hydrogel stayed attached in the microchip and the μEHTs kept beating. Changing the alkaline Tris-HCl buffer to CM medium had the most positive impact on the μEHTs, they never stopped beating after coating and encapsulation. Adding the AP as oxidant seems to help the hydrogel stay attached in the chip for at least 4 days. The UV-vis spectrophotometry experiment showed that adding AP increases the amount of PDA intermediates formed. The water contact angle was 19°which indicates that the PDA coating in CM medium makes PDMS hydrophilic. The pressure experiment has no reliable conclusion because of the high variation, but suggests that the hydrogel is better attached with the DA+AP in CM medium coating.

7 Acknowledgements

First of all I would like to thank Tomas van Dorp for being my daily supervisor and for his excellent guidance and feedback during the assignment.

I also would like to thank my committee chair dr. A.D. van der Meer for giving me the opportunity to perform my bachelor assignment in the Applies Stem cell technologies group.

Furthermore, I would like to thank prof. dr. ir. P. Jonkheijm for being part of the examination committee.

A special thanks goes out to my fellow bachelor students at AST Anna Wolters, Anne Braat, Ceren Kutucu, Krissie Endhoven, Myrthe Pasterkamp and Sacha Bosch for their support.

Finally, I would like to thank the entire AST group for providing a pleasant working environment.

References

[1] Litviňuková M, Talavera-López C, Maatz H, Reichart D, Worth CL, Lindberg EL, et al. Cells of the adult human heart. Nature 2020 588:7838. 2020 9;588(7838):466-72. Available from: https://www.nature.com/articles/s41586-020-2797-4.

[2] Woodcock EA, Matkovich SJ. Cardiomyocytes structure, function and associated pathologies. International Journal of Biochemistry and Cell Biology. 2005;37(9):1746-51.

[3] Marieb EN, Hoehn K. The Cardiovascular System: The Heart. In: Physiology, Human Anatomy &; 2016. p. 683-717.

[4] Ivey MJ, Tallquist MD. Defining the Cardiac Fibroblast: A New Hope. Circulation journal : official journal of the Japanese Circulation Society. 2016 10;80(11):2269. Available from: https://www.ncbi.nlm.nih.gov/pmc/articles/PMC5588900/.

[5] Marieb EN, Hoehn K. Blood. In: Human Anatomy & Physiology; 2016. p. 655-82.

[6] Oliver G, Kipnis J, Randolph GJ, Harvey NL. The Lymphatic Vasculature in the 21st Century: Novel Functional Roles in Homeostasis and Disease. Cell. 2020;182(2):270-96. Available from: https://doi.org/10.1016/j.cell.2020.06.039.

[7] Tammela T, Alitalo K. Lymphangiogenesis: Molecular Mechanisms and Future Promise. Cell. 2010 2;140(4):460-76.

[8] WHO. The top 10 causes of death - Factsheet. WHO reports. 2020;(December 2020):1-9. Available from: https://www.who.int/news-room/fact-sheets/detail/the-top-10-causes-of-death.

[9] Thomas H, Diamond J, Vieco A, Chaudhuri S, Shinnar E, Cromer S, et al. Global Atlas of Cardiovascular Disease 2000-2016: The Path to Prevention and Control. Global Heart. 2018;13(3):143-63.

[10] Hu D, Li L, Li S, Wu M, Ge N, Cui Y, et al. Lymphatic system identification, pathophysiology and therapy in the cardiovascular diseases. Journal of Molecular and Cellular Cardiology. 2019 8;133:99-111. Available from: http://www.jmcc-online.com/article/S0022282819301221/fulltext.

[11] Henderson AR, Choi H, Lee E. Blood and lymphatic vasculatures on-chip platforms and their applications for organ-specific in vitro modeling. Micromachines. 2020;11(2).

[12] Abulaiti M, Yalikun Y, Murata K, Sato A, Sami MM, Sasaki Y, et al. Establishment of a heart-on-a-chip microdevice based on human iPS cells for the evaluation of human heart tissue function. Scientific Reports. 2020;10(1):1-12. Available from: https://doi.org/10.1038/s41598-020-76062-w.

[13] Gaudriault P, Fassini D, Homs-Corbera A. Heart-on-a-chip. Elsevier Inc.; 2019. Available from: http://dx.doi.org/10.1016/B978-0-12-817202-5.00008-5.

[14] Wu Q, Liu J, Wang X, Feng L, Wu J, Zhu X, et al.. Organ-on-a-chip: Recent breakthroughs and future prospects. BioMed Central; 2020. Available from: https://biomedical-engineering-online.biomedcentral.com/articles/10.1186/s12938-020-0752-0.

[15] Wilkinson JM. Need for alternative testing methods and opportunities for organ-on-a-chip systems. In: Organ-on-a-chip. Elsevier Inc.; 2020. p. 1-11. Available from: https://linkinghub.elsevier.com/retrieve/pii/B9780128172025000012.

[16] Leung CM, de Haan P, Ronaldson-Bouchard K, Kim GA, Ko J, Rho HS, et al. A guide to the organ-on-a-chip. Nature Reviews Methods Primers 2022 2:1. 2022 5;2(1):1-29. Available from: https://www.nature.com/articles/s43586-022-00118-6.

[17] James Kirkpatrick C, Fuchs S, Iris Hermanns M, Peters K, Unger RE. Cell culture models of higher complexity in tissue engineering and regenerative medicine. Biomaterials. 2007 12;28(34):5193-8.

[18] Zhang S. Beyond the Petri dish. Nature Biotechnology. 2004 2;22(2):151-2. Available from: http://www.nature.com/articles/nbt0204-151.

[19] Akther F, Little P, Li Z, Nguyen NT, Ta HT. Hydrogels as artificial matrices for cell seeding in microfluidic devices. RSC Advances. 2020;10(71):43682-703.

[20] Shanti A, Hallfors N, Petroianu GA, Planelles L, Stefanini C. Lymph Nodes-On-Chip: Promising Immune Platforms for Pharmacological and Toxicological Applications. Frontiers in Pharmacology. 2021;12(August):1-13.

[21] Sun W, Chen YQ, Luo GA, Zhang M, Zhang HY, Wang YR, et al. Organs-on-chips and Its Applications. Chinese Journal of Analytical Chemistry. 2016 4;44(4):533-41.

[22] Ong CS, Nam L, Ong K, Krishnan A, Huang CY, Fukunishi T, et al. 3D and 4D bioprinting of the myocardium: Current approaches, challenges, and future prospects. BioMed Research International. 2018 4;2018.

[23] Ribeiro MC, Rivera-Arbeláez JM, Cofiño-Fabres C, Schwach V, Slaats RH, Ten Den SA, et al. A New Versatile Platform for Assessment of Improved Cardiac Performance in Human-Engineered Heart Tissues. Journal of Personalized Medicine. 2022;12(2).

[24] Marsano A, Conficconi C, Lemme M, Occhetta P, Gaudiello E, Votta E, et al. Beating heart on a chip: a novel microfluidic platform to generate functional 3D cardiac microtissues. Lab on a Chip. 2016 1;16(3):599-610. Available from: https://pubs-rsc-org.ezproxy2.utwente.nl/en/content/articlelanding/2016/lc/c5lc01356a.

[25] Ribas J, Sadeghi H, Manbachi A, Leijten J, Brinegar K, Zhang YS, et al. Cardiovascular Organ-on-a-Chip Platforms for Drug Discovery and Development. Applied in Vitro Toxicology. 2016 6;2(2):82. Available from: https://www.ncbi.nlm.nih.gov/pmc/articles/PMC5044977/.

[26] Sato M, Sasaki N, Ato M, Hirakawa S, Sato K, Sato K. Microcirculation-on-a-Chip: A Microfluidic Platform for Assaying Blood- and Lymphatic-Vessel Permeability. PLOS ONE. 2015 9;10(9):e0137301. Available from: https://journals.plos.org/plosone/article?id=10.1371/journal.pone.0137301.

[27] Gong MM, Lugo-Cintron KM, White BR, Kerr SC, Harari PM, Beebe DJ. Human organotypic lymphatic vessel model elucidates microenvironment-dependent signaling and barrier function. Biomaterials. 2019;214(November 2018):119225. Available from: https://doi.org/10.1016/j.biomaterials.2019.119225.

[28] Kim S, Chung M, Jeon NL. Three-dimensional biomimetic model to reconstitute sprouting lymphangiogenesis in vitro. Biomaterials. 2016 2;78:115-28.

[29] Osaki T, Serrano JC, Kamm RD. Cooperative Effects of Vascular Angiogenesis and Lymphangiogenesis. Regenerative Engineering and Translational Medicine. 2018;4(3):120-32.

[30] Lv D, Yu SC, Ping YF, Wu H, Zhao X, Zhang H, et al. A three-dimensional collagen scaffold cell culture system for screening anti-glioma therapeutics. Oncotarget. 2016 7;7(35):56904-14. Available from: https://www.oncotarget.com/article/10885/text/.

[31] Ahmed EM. Hydrogel: Preparation, characterization, and applications: A review. Journal of Advanced Research. 2015;6(2):105-21. Available from: http://dx.doi.org/10.1016/j.jare.2013.07.006.

[32] Antoine EE, Vlachos PP, Rylander MN. Review of collagen i hydrogels for bioengineered tissue microenvironments: Characterization of mechanics, structure, and transport. Mary Ann Liebert, Inc.; 2014. Available from: https://www.ncbi.nlm.nih.gov/pmc/articles/PMC4241868/.

[33] Janmey PA, Winer JP, Weisel JW. Fibrin gels and their clinical and bioengineering applications. The Royal Society; 2009. Available from: https://www.ncbi.nlm.nih.gov/pmc/articles/PMC2575398/.

[34] Cholewinski E, Dietrich M, Flanagan TC, Schmitz-Rode T, Jockenhoevel S. Tranexamic acid-an alternative to aprotinin in fibrin-based cardiovascular tissue engineering. Tissue Engineering - Part A. 2009 11;15(11):3645-53. Available from: https://pubmed.ncbi.nlm.nih.gov/19496679/.

[35] Qiu Y, Ahn B, Sakurai Y, Hansen CE, Tran R, Mimche PN, et al. Microvasculature-on-a-chip for the long-term study of endothelial barrier dysfunction and microvascular obstruction in disease. Nature Biomedical Engineering. 2018 6;2(6):453-63. Available from: https://pubmed.ncbi.nlm.nih.gov/30533277/.

[36] Ding C, Chen X, Kang Q, Yan X. Biomedical Application of Functional Materials in Organ-on-a-Chip. Frontiers Media SA; 2020. Available from: https://www.ncbi.nlm.nih.gov/pmc/articles/PMC7387427/.

[37] van Meer BJ, de Vries H, Firth KSA, van Weerd J, Tertoolen LGJ, Karperien HBJ, et al. Small molecule absorption by PDMS in the context of drug response bioassays. Biochemical and Biophysical Research Communications. 2017 1;482(2):323-8.

[38] Gökaltun A, Kang YBA, Yarmush ML, Usta OB, Asatekin A. Simple Surface Modification of Poly(dimethylsiloxane) via Surface Segregating Smart Polymers for Biomicrofluidics. Scientific Reports. 2019;9(1). Available from: www.nature.com/scientificreports.

[39] Park SE, Georgescu A, Oh JM, Kwon KW, Huh D. Polydopamine-Based Interfacial Engineering of Extracellular Matrix Hydrogels for the Construction and Long-Term Maintenance of Living Three-Dimensional Tissues. ACS Applied Materials and Interfaces. 2019;11(27):23919-25.

[40] Ryu JH, Messersmith PB, Lee H. Polydopamine Surface Chemistry: A Decade of Discovery. ACS Applied Materials and Interfaces. 2018;10(9):7523-40.

[41] Lee H, Dellatore SM, Miller WM, Messersmith PB. Polydopamine Coating. Science. 2008;318(5849):426-30.

[42] Wang Z, Yang HC, He F, Peng S, Li Y, Shao L, et al. Mussel-Inspired Surface Engineering for Water-Remediation Materials. Matter. 2019;1(1):115-55. Available from: https://doi.org/10.1016/j.matt.2019.05.002.

[43] Cortés MT, Vargas C, Blanco DA, Quinchanegua ID, Cortés C, Jaramillo AM. Bioinspired Polydopamine Synthesis and Its Electrochemical Characterization. Journal of Chemical Education. 2019;96(6):1250-5.

[44] Lakshminarayanan R, Madhavi S, Sim CPC. Oxidative Polymerization of Dopamine: A High-Definition Multifunctional Coatings for Electrospun Nanofibers - An Overview. In: Dopamine - Health and Disease. IntechOpen; 2018. Available from: https://www.intechopen.com/chapters/63723.

[45] Wei Q, Zhang F, Li J, Li B, Zhao C. Oxidant-induced dopamine polymerization for multifunctional coatings. Polymer Chemistry. 2010;1(9):1430-3.

[46] Hong SH, Hong S, Ryou MH, Choi JW, Kang SM, Lee H. Sprayable Ultrafast Polydopamine Surface Modifications. Advanced Materials Interfaces. 2016;3(11).

[47] Salomäki M, Marttila L, Kivelä H, Ouvinen T, Lukkari J. Effects of pH and Oxidants on the First Steps of Polydopamine Formation: A Thermodynamic Approach. Journal of Physical Chemistry B. 2018;122(24):6314-27.

[48] Park JP, Song IT, Lee J, Ryu JH, Lee Y, Lee H. Vanadyl-catecholamine hydrogels inspired by ascidians and mussels. Chemistry of Materials. 2015;27(1):105-11.

[49] Wei Q, Zhang F, Li J, Li B, Zhao C. Supplementary Material (ESI) for Oxidant-induced dopamine polymerization for multifunctional coatings Supporting Information. Polymer Chemistry. 2010;19(c).

[50] Ribeiro MC, Slaats RH, Schwach V, Rivera-Arbelaez JM, Tertoolen LGJ, van Meer BJ, et al. A cardiomyocyte show of force: A fluorescent alpha-actinin reporter line sheds light on human cardiomyocyte contractility versus substrate stiffness. Journal of Molecular and Cellular Cardiology. 2020 4;141:54-64. Available from: http://www.jmcc-online.com/article/S0022282820300699/fulltext.

[51] Lamaoui A, Palacios-Santander JM, Amine A, Cubillana-Aguilera L. Molecularly imprinted polymers based on polydopamine: Assessment of non-specific adsorption. Microchemical Journal. 2021;164(January).

[52] Chuah YJ, Koh YT, Lim K, Menon NV, Wu Y, Kang Y. Simple surface engineering of polydimethylsiloxane with polydopamine for stabilized mesenchymal stem cell adhesion and multipotency. Scientific Reports. 2015;5(November):1-12.

[53] Ponzio F, Barthès J, Bour J, Michel M, Bertani P, Hemmerlé J, et al. Oxidant Control of Polydopamine Surface Chemistry in Acids: A Mechanism-Based Entry to Superhydrophilic-Superoleophobic Coatings. Chemistry of Materials. 2016;28(13):4697-705.

[54] Ku SH, Ryu J, Hong SK, Lee H, Park CB. General functionalization route for cell adhesion on non-wetting surfaces. Biomaterials. 2010 3;31(9):2535-41. Available from: https://pubmed.ncbi.nlm.nih.gov/20061015/.

[55] Von Euler H, Söderstedt A, Thörne A, Olsson JM, Yongqing G. Cellular toxicity induced by different pH levels on the R3230AC rat mammary tumour cell line. An in vitro model for investigation of the tumour destructive properties of electrochemical treatment of tumours. Bioelectrochemistry (Amsterdam, Netherlands). 2002;58(2):163-70. Available from: https://pubmed.ncbi.nlm.nih.gov/12414322/.

[56] Kašpárková V, Humpoliček P, Stejskal J, Capáková Z, Bober P, Skopalová K, et al. Exploring the critical factors limiting polyaniline biocompatibility. Polymers. 2019;11(2).

[57] idenTx 3 Chip - AIM Biotech;. Available from: https://aimbiotech.com/product/identx-3-chip/.

8 Appendix

8.1 Components cardiomyocyte culture medium

Component	Concentration	Fabricant, catalog number
Glucose	15 mM	Millipore, 1083371000
Lactate	0.718 μL/mL	unk
T3	100 nM	Sigma, T6397-100G
Dexamethasone	1 μM	Tocris, 1126/100
IGF1	100 ng/ml	Sigma, I1271
FGF2 (for CFs only)	50 ng/ml	Miltenyi Biotec, 130-104-922

Table 2: Components CM and CF culture medium are added to base medium.

8.2 Components cell-gel mixture

Component	Concentration (μg/mL)	Fabricant, catalog number
Fibrinogen	2000	Sigma-Aldrich, F8630
Matrigel	1000	VWR, 356252
Aprotonin	2.5	Sigma-Aldrich, A1153
Thrombin	0.6 U/mL	Sigma-Aldrich, T7513-100UN

Table 3: Components of cell-gel mixture are added to CM medium with cells.

8.3 Components hydrogel

Component	Concentration (μg/mL)	Fabricant, catalog number
Fibrinogen	3000	Sigma-Aldrich, F8630
Collagen I	200	Thermo Scientific, A1048301
Aprotonin	3.75	Sigma-Aldrich, A1153
Thrombin	0.9 U/mL	Sigma-Aldrich, T7513-100UN

Table 4: Components of hydrogel are added to CM medium or PBS depending on the experiment.

8.4 UV-vis spectra all conditions

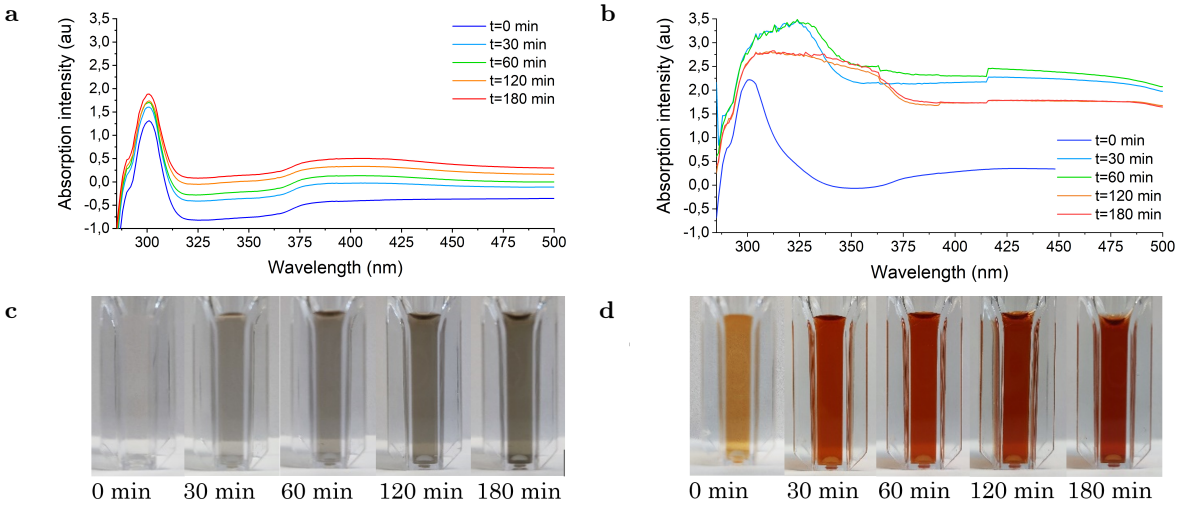

Figure 11: UV-vis spectra (a) and color change (c) of DA in a Tris-HCl pH 8.55 buffer over 3 hours time. UV-vis spectra (b) and color change (d) of DA mixed with AP in a Tris-HCl pH 8.55 buffer over 3 hours time.

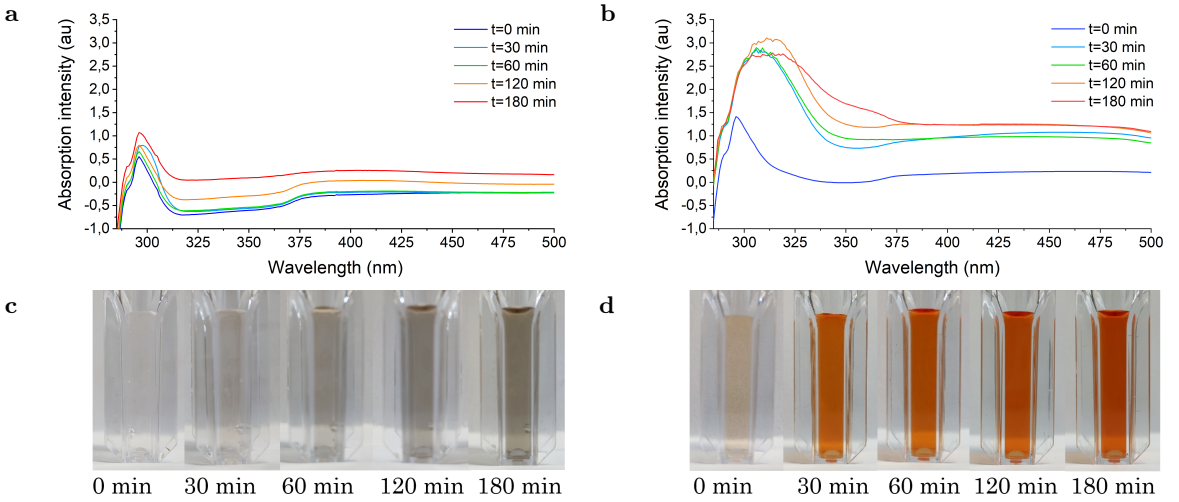

Figure 12: UV-vis spectra (a) and color change (c) of DA in a Tris-HCl pH 7.93 buffer over 3 hours time. UV-vis spectra (b) and color change (d) of DA mixed with AP in a Tris-HCl pH 7.94 buffer over 3 hours time.

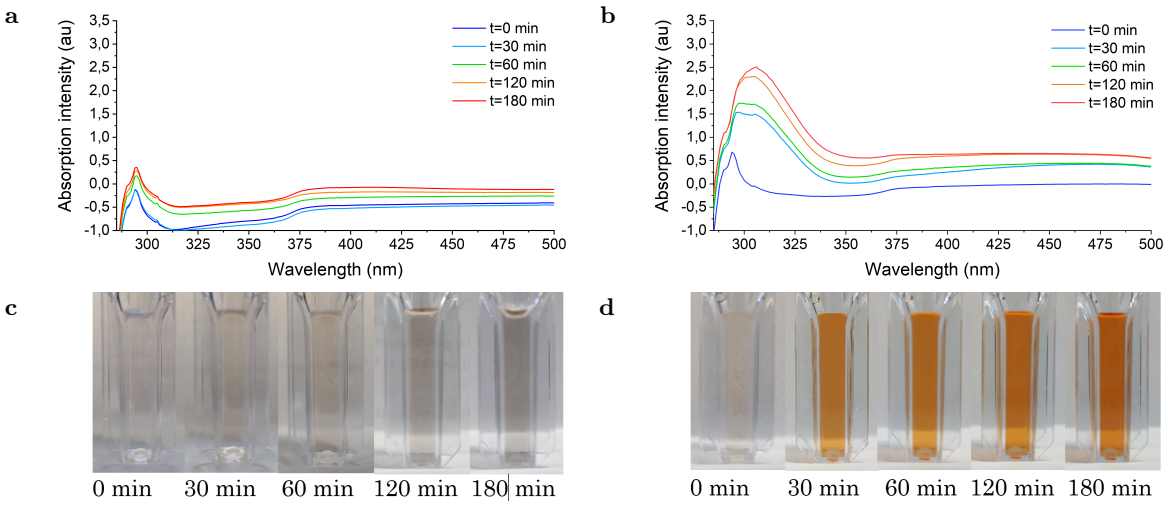

Figure 13: UV-vis spectra (a) and color change (c) of DA in a Tris-HCl pH 7.51 buffer over 3 hours time. UV-vis spectra (b) and color change (d) of DA mixed with AP in a Tris-HCl pH 7.51 buffer over 3 hours time.

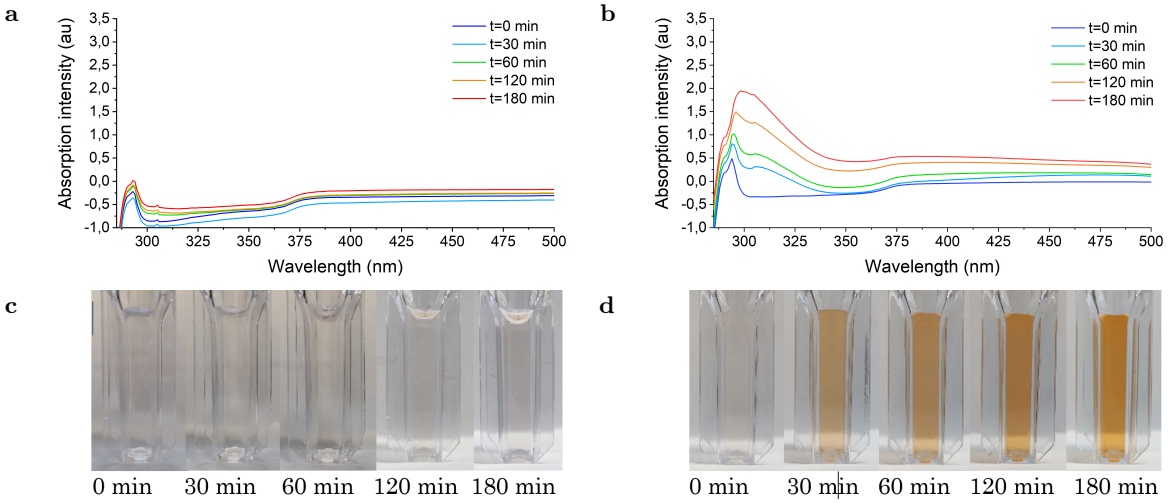

Figure 14: UV-vis spectra (a) and color change (c) of DA in a Tris-HCl pH 7.06 buffer over 3 hours time. UV-vis spectra (b) and color change (d) of DA mixed with AP in a Tris-HCl pH 7.00 buffer over 3 hours time.

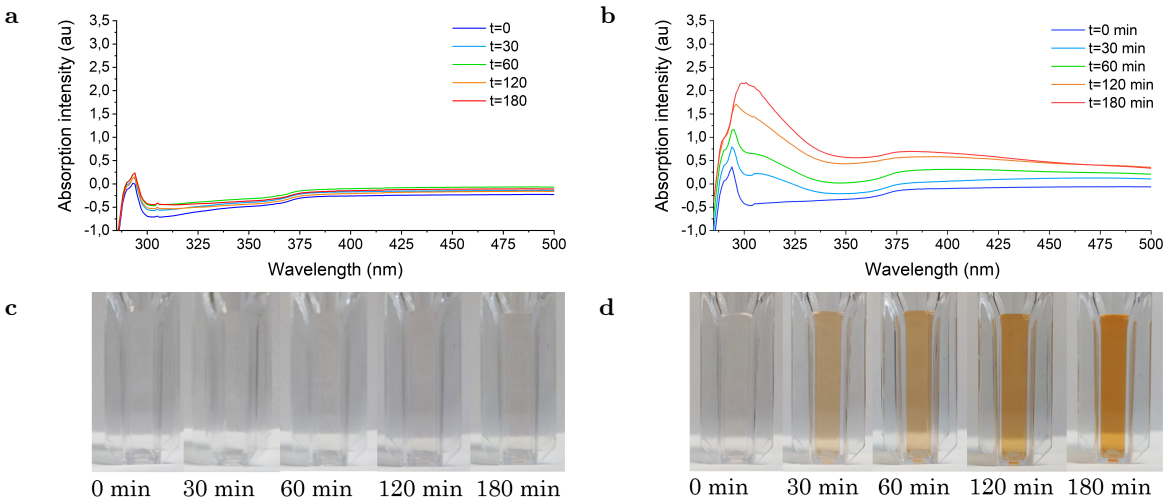

Figure 15: UV-vis spectra (a) and color change (c) of DA in a Tris-HCl pH 6.87 buffer over 3 hours time. UV-vis spectra (b) and color change (d) of DA mixed with AP in a Tris-HCl pH 6.87 buffer over 3 hours time.

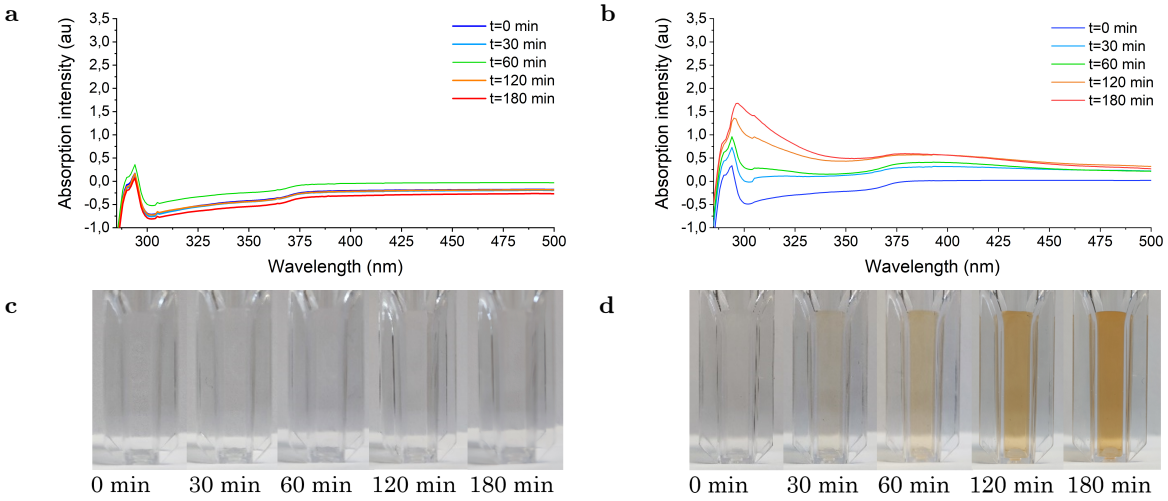

Figure 16: UV-vis spectra (a) and color change (c) of DA in a Tris-HCl pH 5.90 buffer over 3 hours time. UV-vis spectra (b) and color change (d) of DA mixed with AP in a Tris-HCl pH 5.75 buffer over 3 hours time.

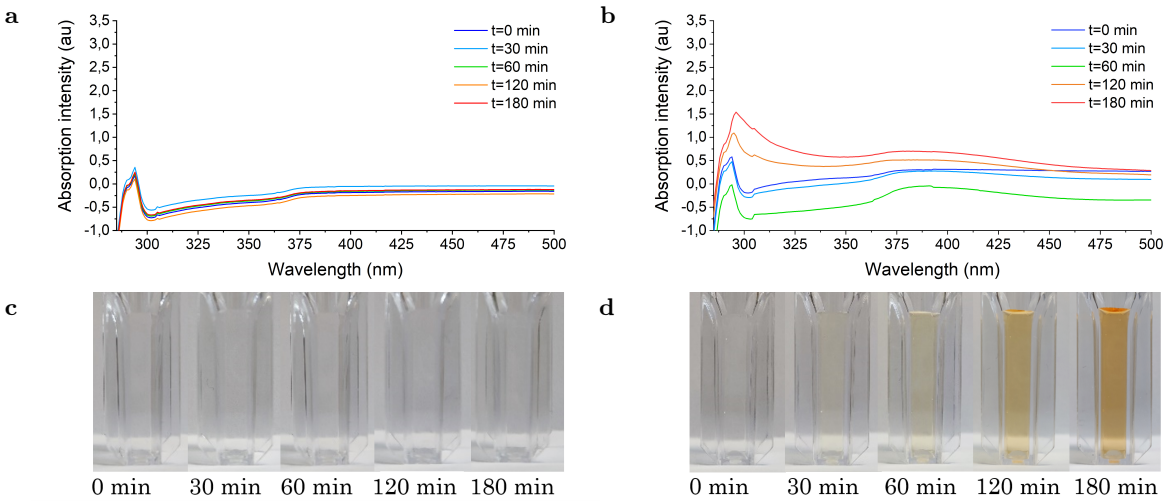

Figure 17: UV-vis spectra (a) and color change (c) of DA in a Tris-HCl pH 2.61 buffer over 3 hours time. UV-vis spectra (b) and color change (d) of DA mixed with AP in a Tris-HCl pH 2.66 buffer over 3 hours time.

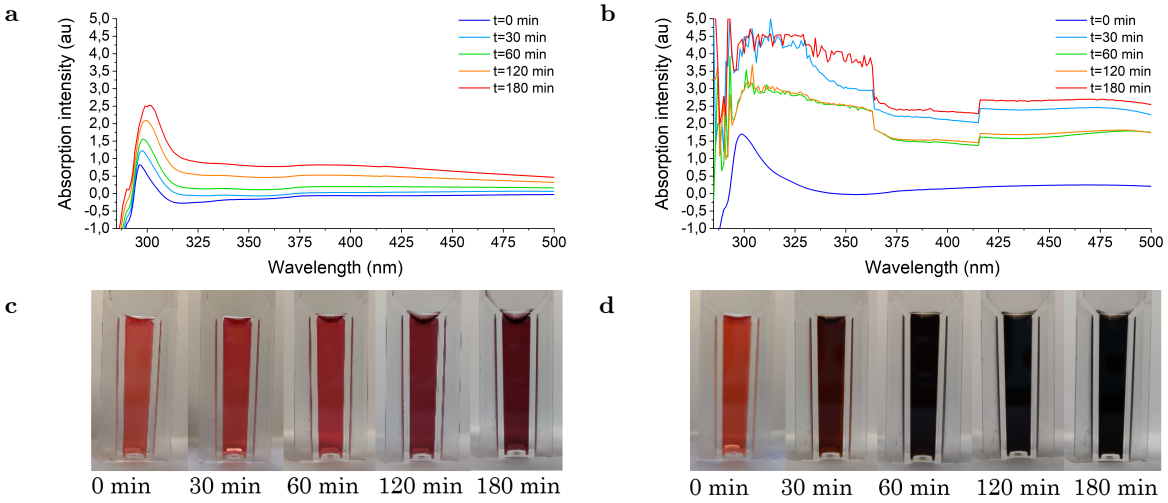

Figure 18: UV-vis spectra (a) and color change (c) of DA in CM medium pH 7.3 buffer over 3 hours time. UV-vis spectra (b) and color change (d) of DA mixed with AP in CM medium pH 7.3 buffer over 3 hours time.

8.5 Contact angle measurements all conditions

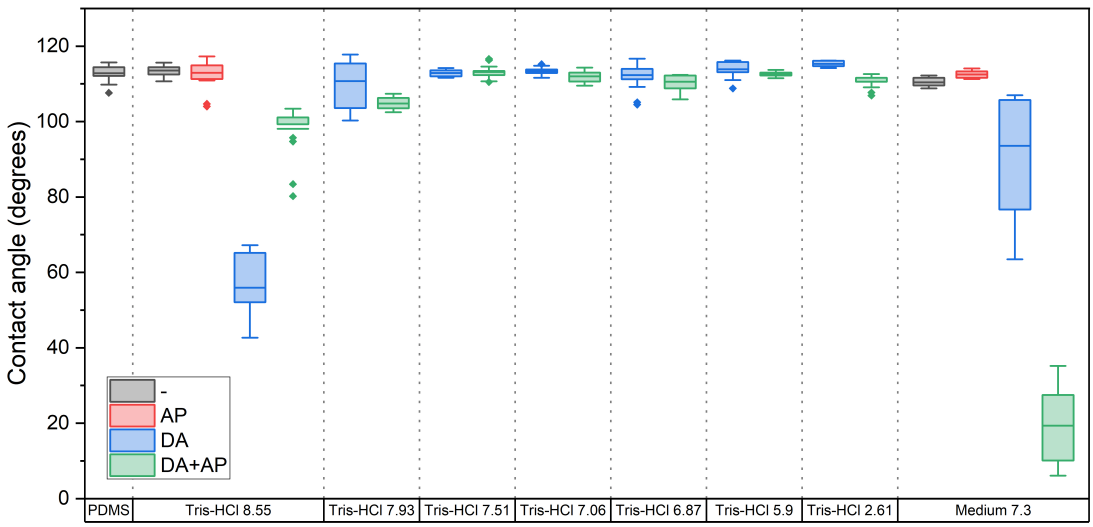

Figure 19: Water contact angle of all conditions. The error bars are the SD and the diamond shapes mark the outliers.

8.6 PrestoBlue metabolic activity assay all results

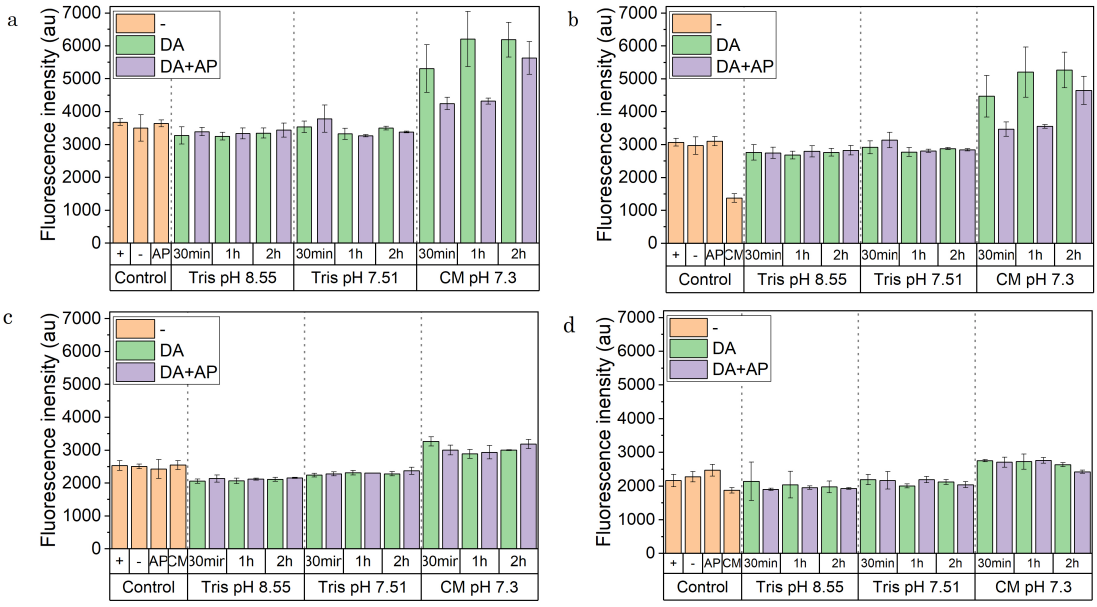

Figure 20: Fluorescence intensity of the PrestoBlue metabolic activity assay under different coating conditions measured at 0 hours (a), 2 hours (b), 4 hours (c) and 24 hours (d) after coating. The orange bars are the controls: + is the positive control consisting of only CM medium, - is the negative control where saponin is added, AP means only AP with CM medium is used and CM is CM medium with PrestoBue.

8.7 µEHTs in microchip

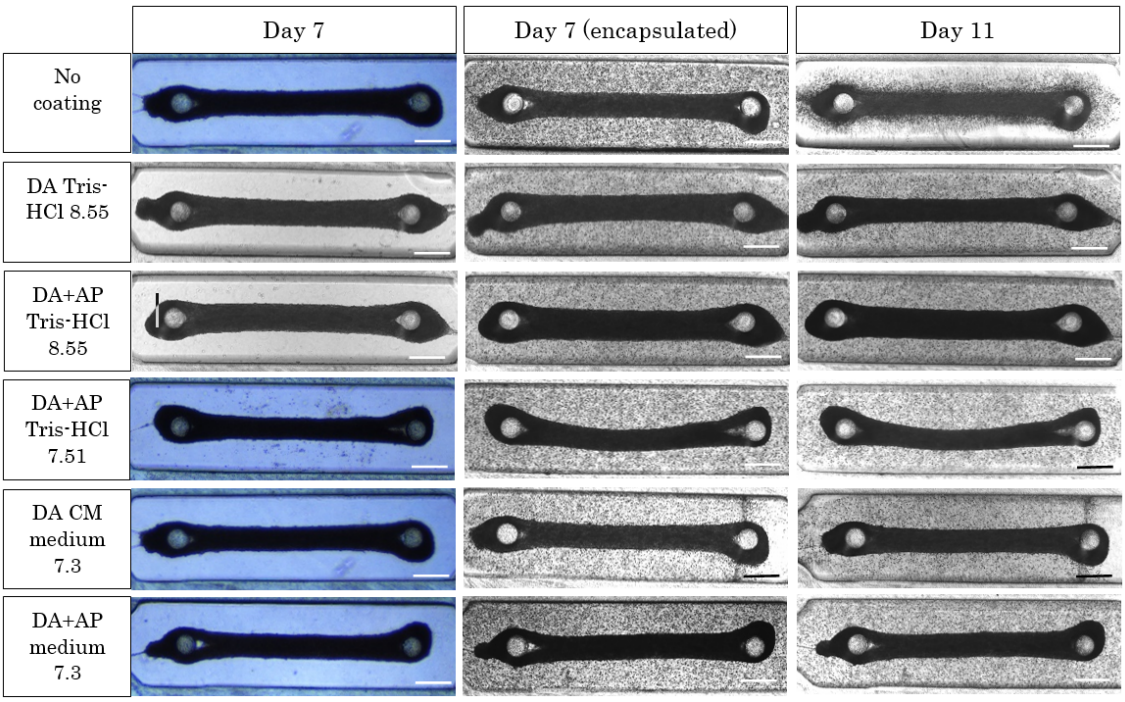

Figure 21: Fefore and after hydrogel encapsulation images on day 7 of the μEHTs cultured on chip. The chips were coated and the tissues were encapsulated with hydrogel with beads. Chips were uncoated **(a)**, coated with DA **(b)** and DA+AP **(c)** in Tris-HCl with pH 8.55 for 30 minutes, DA+AP **(d)** in Tris-HCl with pH 7.51 for 60 minutes and DA **(e)** and DA+AP **(f)** in CM medium pH 7.3. Scale bars: 500 μm.